Minimum FGF2 Binding Structural Requirements of Heparin and Heparan Sulfate Oligosaccharides As Determined by NMR Spectroscopy[†]

Sara Guglieri,[‡] Miloš Hricovíni,[§] Rahul Raman,[||] Laura Polito,[⊥] Giangiacomo Torri,[‡] Benito Casu,[‡] Ram Sasisekharan,[||] and Marco Guerrini*[,‡]

G. Ronzoni Institute for Chemical and Biochemical Research, Milan, Italy, Institute of Chemistry, Slovak Academy of Sciences, Bratislava, Slovakia, Department of Biological Engineering, Harvard-MIT Division of Health Sciences and Technology, Massachusetts Institute of Technology, Cambridge, Massachusetts 02139, and Department of Organic and Industrial Chemistry, University of Milan, Milan, Italy

Received May 28, 2008; Revised Manuscript Received October 23, 2008

ABSTRACT: Heparin and heparan sulfate (HS) glycosaminoglycans (HSGAGs) are sulfated polysaccharides that play important roles in fundamental biological processes by binding to proteins. The prototypic example of HSGAG−protein interactions is that with the fibroblast growth factors (FGFs), specifically FGF1 and FGF2. Structural and biochemical studies have shown that the chain length, sulfation pattern, and conformation of HSGAGs play a critical role in FGF binding and activity. Previously, we showed that a tetrasaccharide of the form $A_{NS,6X}$-I_{2S}-$A_{NS,6X}$-I_{2S}-OPr (where X is OH or O-sulfate and Pr is propyl) with at least one of the $A_{NS,6X}$ residues having a 6-O sulfate group was the minimum binding motif for FGF1 [Guerrini, M., Agulles, T., Bisio, A., Hricovini, M., Lay, L., Naggi, A., Poletti, L., Sturiale, L., Torri, G., and Casu, B. (2002) *Biochem. Biophys. Res. Commun. 292*, 222−230]. We report NMR structural analysis using two-dimensional NOE spectroscopy (2D-NOESY) and transferred NOESY (trNOESY) on a non-6-O-sulfated synthetic tetrasaccharide TETRA (A_{NS}-I_{2S}-A_{NS}-I_{2S}-OPr) both in its free state and bound to FGF2. This tetrasaccharide comprises both the structural trisaccharide motif A_{NS}-I_{2S}-A_{NS} that forms "kinks" in longer heparin chains induced by FGF binding [Raman, R., Venkataraman, G., Ernst, S., Sasisekharan, V., and Sasisekharan, R. (2003) *Proc. Natl. Acad. Sci. U.S.A. 100*, 2357−2362] and the common binding motif I_{2S}-A_{NS}-I_{2S} present in octasaccharides that exhibited strong FGF2 binding [Kreuger, J., Salmivirta, M., Sturiale, L., Gimenez-Gallego, G., and Lindahl, U. (2001) *J. Biol. Chem. 276*, 30744−30752]. These data suggest that TETRA could be the shortest HSGAG oligosaccharide that binds to FGF2. Furthermore, our study confirms that both the IdoA residues in TETRA adopt the chair $^1C_4$ conformation upon FGF2 binding to provide the best molecular fit in contrast to an analogous 6-O-sulfated tetrasaccharide motif observed in the FGF2−HSGAG cocrystal structure where one of the IdoAs adopts skew-boat ^2S_O conformation. Thus, our study highlights the fact that the conformational plurality of IdoA is able to accommodate the changes in the sulfation pattern to provide the necessary specificity for protein binding.

HSGAGs[1] are complex polysaccharides that are characterized by a disaccharide repeat unit of α-GlcN linked 1 → 4 to a uronic (α-IdoA/β-GlcA) acid. Heterogeneity within the HSGAG polysaccharide arises from the number of disaccharide repeat units present, as well as four potential sites for chemical modification in the form of acetylation or sulfation at the N position of the glucosamine and sulfation at the 2-O position of the uronic acid and the 3-O and 6-O positions of the glucosamine (*1*−*3*). It is becoming increasingly evident that unique HSGAG sequences specifically bind to a wide range of proteins (*4*−*7*), including morphogens (*8, 9*), growth factors (*4, 10, 11*), and enzymes (*12*), and modulate their activity and thereby play an important role in fundamental biological processes. Hence, it is important to understand what governs the specificity of HSGAG−protein interactions. One of the best-studied examples of HSGAG−protein interactions is that of HSGAG−FGF interactions (specifically FGF1 and FGF2) and their role in FGF signaling pathway. The overall mechanism of FGF signaling involves binding of FGF to cell surface HSGAGs which act as coreceptors to facilitate FGF oligomerization and binding of FGF to its tyrosine kinase receptors (FGFRs), leading to FGFR oligomerization and signaling (*10, 13*−*16*). Several studies proposed the FGF oligomerization as a key step that favors the formation of ternary complexes with FGFRs (*17*). However, it was shown that mitogenic activity can be induced

[†] This work was supported by NIH Grant HL-59966.

* To whom correspondence should be addressed. E-mail: guerrini@ronzoni.it. Fax: (+39) 02 70 64 16 34. Phone: (+39) 02 70 64 16 27.

[‡] G. Ronzoni Institute for Chemical and Biochemical Research.

[§] Slovak Academy of Sciences.

[||] Massachusetts Institute of Technology.

[⊥] University of Milan.

[1] Abbreviations: HSGAG, heparin and heparan sulfate glycosaminoglycans; IdoA or I, α-L-iduronic acid; GlcA or G, β-D-glucuronic acid; GlcN or A, α-D-glucosamine; 2S, sulfation at the 2-O position of the uronic acid; 6S, NS, and 3S, sulfation at the 6-O, N, and 3-O positions of the glucosamine, respectively; OPr, propyl group at the reducing end; nr, nonreducing end; r, reducing end; FGF, fibroblast growth factor; FGFR, FGF receptor; NOE, nuclear Overhauser effect; tr-NOE, transferred NOE; NOESY, NOE spectroscopy.

10.1021/bi801007p CCC: $40.75
Published on Web 12/04/2008

with a derivative having sulfate groups on only one side of the oligosaccharide chain, without dimerization (*18, 19*).

The chain length, sulfation pattern, and conformation of HSGAGs are critical determinants of regulation of FGF activity by HSGAGs. HSGAG chains of sufficient length facilitate FGF oligomerization and FGF−FGFR binding (*15*−*17, 20, 21*). On the other hand, exogenous heparin and shorter HSGAG oligosaccharides displace FGFs from FGF−HSGAG−FGFR complexes (*22*), thereby potentially playing an inhibitory role in FGF activity. Structural studies on HSGAG oligosaccharides point to a helical structure with 2_1 symmetry (*23, 24*). Furthermore, the IdoA pyranose ring is conformationally flexible as it can adopt multiple equienergetic conformations such as $^1C_4$, ^2S_O, and, less frequently in heparin sequences, $^4C_1$ forms (*23, 25, 26*). When protein binds, a kink is introduced into the polysaccharide helical structure as pointed out by the analysis of cocrystal structures involving oligosaccharides longer than a tetrasaccharide (*27*). The minimal FGF binding site on HSGAG appears to span a tetrasaccharide chain length comprising a trisaccharide "kink motif" of $A_{NS,6S/OH}$-I_{2S}-$A_{NS,6S/OH}$ and another IdoA residue at the reducing or nonreducing end of the kink (*27*). In the case of both FGF1 and FGF2, the NS and 2S groups together with the $^1C_4$ conformation of the IdoA in this kink motif provide maximum contact with the protein. However, the distinction in the nature of interactions of this minimal tetrasaccharide between FGF1 and FGF2 appears to be the 6S group of $A_{NS,6S}$ and the conformation of the IdoA residue outside the kink sequence. On the basis of the FGF−HSGAG oligosaccharide cocrystal structures (*28, 29*), while in FGF1, the 6S group makes optimal contact with the protein, in FGF2, the 6S group is not involved in the binding, as further demonstrated by biochemical studies (*30*). Moreover, the IdoA residue outside the kink sequence adopts the $^1C_4$ or ^2S_O conformation when bound to FGF1 or FGF2, respectively. The plurality of IdoA conformations and the distinct interactions of the 6S group observed in the FGF−HSGAG cocrystal structures raise a key question about the relationship of 6-O sulfation and IdoA conformation in determining the minimal FGF2 binding HSGAG motif.

The heparin-derived oligosaccharide investigated in most detail as an FGF2 ligand is the 6-O-sulfated hexasaccharide ΔHEXA (Figure 1a), featuring an unsaturated uronic acid residue at the nonreducing terminal and containing both the kink motif ($A_{NS,6S/OH}$-I_{2S}-$A_{NS,6S/OH}$) and the FGF2-binding motif (I_{2S}-$A_{NS,6S/OH}$-I_{2S}). Analysis of the X-ray cocrystal structure (*29*) of the FGF2−ΔHEXA complex indicated that the two sulfate groups circled in Figure 1 (the NSO_3 group of the first $GlcN_{NS,6S}$ residue and the $2SO_3$ group of the first I_{2S} residue) are involved in the closest contacts with amino acid residues of the proteins (namely, Arg120, Lys125, Gln134, Lys135, and Ala136). Furthermore, this analysis also indicated that the terminal residues of the hexasaccharide are only marginally involved in contacts with FGF2, suggesting that tetrasaccharide is likely to be the minimal chain length for FGF2 binding. The FGF2−ΔHEXA cocrystal structure was the first example in which two I_{2S} residues within the protein-bound oligosaccharide adopted two different conformations. The first I_{2S} residue (from the nonreducing end) adopts the $^1C_4$ form, and the second I_{2S} residue (outside the high-affinity FGF binding region closer to the reducing end) adopts the ^2S_O form (*29*). In the free state,

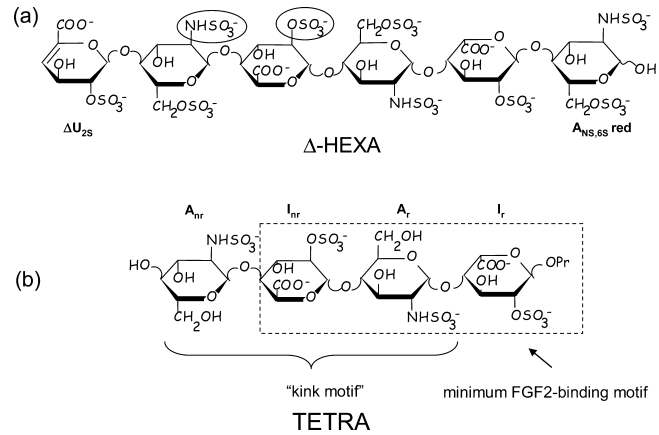

FIGURE 1: Structures of 6-O-sulfated hexasaccharide Δ-HEXA (*27*) (a) and non-6-*O*-sulfated tetrasaccharide TETRA (*33*) (b). Circled groups displayed the strongest contact with FGF2 residues in the X-ray structure (*29*): A_{nr}, $GlcN_{NS}$ bearing the nonreducing disaccharide moiety; I_{nr}, $IdoA_{2S}$ bearing the nonreducing disaccharide moiety; A_r, $GlcN_{NS}$ bearing the reducing disaccharide moiety; I_r, $IdoA_{2S}$ bearing the reducing disaccharide moiety. The kink motif ($A_{NS,6S/OH}$-I_{2S}-$A_{NS,6S/OH}$) and the minimum FGF2-binding motif (I_{2S}-$A_{NS,6S,OH}$-I_{2S}) are highlighted on the TETRA structure.

these two IdoA residues instead exist in equilibrium between the $^1C_4$ and ^2S_O forms (*26, 31*).

The synthetic tetrasaccharide TETRA (A_{NS}-I_{2S}-A_{NS}-I_{2S}) (*32*) (Figure 1b), representing the non-6-O-sulfated core of ΔHEXA, also contains both the kink motif and the minimum FGF2-binding motif. A recent NMR study demonstrated that TETRA does not interact with FGF1 and confirmed the essential role of 6-O-sulfate groups for binding with FGF1 (*33*).

In this study, we performed a conformational analysis of TETRA both in its free state and bound to FGF2 using two-dimensional NOE spectroscopy (NOESY) and transferred NOESY (trNOESY). Our analysis demonstrated the occurrence of the binding, defining NS and 2S groups in an A-I-A-I tetrasaccharide backbone as the minimal structural requirements for the FGF2-binding HSGAG motif. Furthermore, it indicated that, in contrast to what was observed for ΔHEXA in the crystal structure (*29*), the $^1C_4$ conformation is selected by FGF2 for both IdoA residues. Our study also highlights an important relationship between HSGAG IdoA conformation and sulfation pattern where the conformational "flexibility" of the IdoA accommodates the absence of the 6S group to provide the necessary specificity for FGF1 binding.

EXPERIMENTAL PROCEDURES

NMR Experiments. Proton and two-dimensional NOESY spectra of tetrasaccharide both in its free state and bound to FGF2 (tetrasaccharide:FGF2 ratio of 10:1) were obtained at 750 MHz with a Bruker Avance^z 750 spectrometer equipped with a 5 mm TXI probe. All experiments were conducted at 9 °C, except for one proton spectrum of free ligand, which was recorded at 40 °C to better resolve $^3J_{HH}$ coupling constants. Two-dimensional phase-sensitive NOESY and transferred-NOESY spectra of the ligand in its free and FGF2-complexed state were recorded using a standard pulse sequence.

For both free and bound studies, samples were dissolved in 10 mM phospate buffer and 0.1 M NaCl (pH 6.0 in

99.996% D_2O). Presaturation of the HDO resonance was achieved by low-power irradiation during the relaxation delay and the mixing time. A total of 32 transients were collected for each free induction decay. NOESY spectra were obtained with two and three different mixing times for the free and bound tetrasaccharide, respectively, using a relaxation delay of 2 s. The spectral width was 1700 Hz, and data (matrix size of 2048 × 320 points) were zero-filled to 2K × 1K before Fourier transformation and multiplied with a shifted (π/2) squared cosine function.

Computational Procedures. All calculations were carried out using the MACROMODEL 7.1 version of BATCHMIN on a SGO2 workstation. The force field used was all atoms AMBER* which includes Homan's parameters for pyranose (*34*). The GB/SA (Generalized Born/Surface Area) continuum water solvation model was used (*35*). To avoid IdoA ring distortions, all iduronic rings were locked in the suitable conformation by constraints on H2−H5 and H5−H4 distances.

Two tetrasaccharide starting models, differing in the I_r geometry (adopting the $^1C_4$ or ^2S_O form), were obtained from the heparin model (*36*). The I_{nr} residue was considered to be in the $^1C_4$ conformation. Subsequently, 4000 steps of Monte Carlo/energy minimization (MC/EM) (*37, 38*) were performed on these optimized models.

The lowest-energy minima of the two models were then used to calculate time-averaged NOEs using a full relaxation matrix by NOEPROM (available at http://desoft03.usc.es/rmnweb/rmnexp_software.html#noeprom). The ratio of $^1C_4$ and ^2S_O forms used in calculation was 80:20.

The model of the starting FGF2 tetrasaccaride was obtained by suitably modifying the FGF2 hexasaccaride structure (Protein Data Bank entry 1BFC) (*29*). In all starting structures, A_{nr} and A_r residues were in the $^4C_1$ conformation and the I_{nr} residue was in the $^1C_4$ conformation as in the X-ray structure (*29*). Three SD simulations were run starting from tetrasaccharide models constraining I_r residues in the ^2S_O, $^1C_4$, and $^4C_1$ conformations. In starting geometries of all three models, φ and ψ torsions of the $A_{nr}I_r$ glycosidic linkage were maintained at the same values of the X-ray hexasaccaride structure, consistent with published data (*36, 39, 40*). All calculations were carried out on complex substructures, including the saccharide and all the protein atoms within 15 Å of the ligand. In this way, the saccharide atoms were considered freely moving atoms, whereas the protein atoms were anchored by a harmonic restraining force constant of 418 kJ mol^{-1} $Å^{-2}$ at the periphery of the freely moving substructure. Moreover, to lock the ligand at the binding site distance, constraints were imposed between the binding disaccharide moiety and the amino acid residue interacting with it, with respect to polar contacts found out in X-ray structures (*29*). Geometries of three substructures were optimized by energy minimization (EM). On each optimized model, a 400 ps SD simulation was run using a constant temperature of 300 K with a bath thermal constant (τ) of 0.2 ps and a dynamic time step of 1.0 fs. Obtained conformers were then optimized by EM.

Theoretical tr-NOEs of the tetrasaccharide in dynamic exchange between free and FGF2-bound states were calculated, on molecular models thus obtained, by CORCEMA (*41*). The correlation time of FGF2 was considered as isotropic and estimated from published data (*42*) (τ_{FGF2} = 13 ns), whereas an average correlation time value characteristic of oligosaccarides having a similar structure was used for TETRA (τ_{BB} = 0.6 ns) (*33*). Starting from FGF1-tetrasaccharide complex data (*33*), we then estimated the values of K_d and k_{off} to yield the best agreement with experimental NOEs ($K_d = 4 \times 10^{-5}$ M; $k_{off} = 50$ s^{-1}). Fitting between experimental and theoretical NOEs was evaluated by computing R factors according to the formula $R = \{\sum[I_{ij}^{exp}(\tau_{mix}) - I_{ij}^{calc}(\tau_{mix})]^2/\sum[I_{ij}^{exp}(\tau_{mix})]^2\}^{1/2}$, where I_{ij}^{exp} values are the experimental cross-peak intensities, I_{ij}^{calc} values are the calculated cross-peak intensities, and τ_{mix} are the mixing times.

Table 1: Refined Experimental $^3J_{HH}$ Coupling Constants (rows 2 and 3) and Computed Time-Averaged (80:20 $^1C_4$:$^2S_0$ ratio) Values (row 5) for the I_r Residue in TETRA (40 °C, 750 MHz) in the Free State[a]

	$J_{1,2}$	$J_{2,3}$	$J_{3,4}$	$J_{4,5}$
I_{nr}	1.7	3.9	3.6	2.3
I_r	2.5	4.8	3.8	2.7
I_{nr}_calc	1.7	3.0	3.1	2.3
I_r_calc	2.3	4.5	3.4	2.7

[a] I_{nr} (row 4) was considered to be in the $^1C_4$ conformation exclusively (*45*).

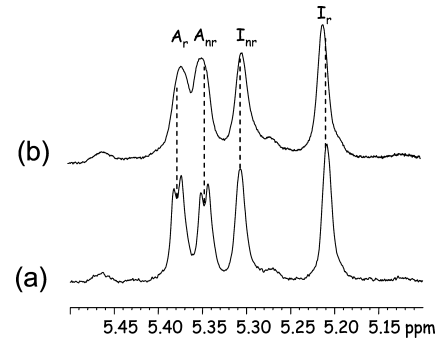

FIGURE 2: Partial ^1H NMR spectra (750 MHz, 9 °C) of TETRA in its free state (a) and bound to FGF2 (b).

RESULTS

Conformational Analysis of the Free TETRA in Solution. The $^3J_{HH}$ values (Table 1; the partial ^1H spectrum shown in Figure 2a) of the unbound tetrasaccharide indicate that the $IdoA_{2S}$ of the nonreducing disaccharide (I_{nr}) is present almost exclusively in the $^1C_4$ conformation. Somewhat larger coupling constants measured in the reducing end IdoA (I_r) residue indicate that a small percentage of the ^2S_O form contributes to the conformational equilibrium of tetrasaccharide (*26, 43−45*). Comparison of computed time-averaged $^3J_{HH}$ values with experimental data suggested that the $^1C_4$:^2S_O ratio is approximately 80:20. This result is further supported by 2D-NOESY spectra (Figure 3a and Table 2a). The small H5−H2 cross-peak (1.0%, 150 ms mixing time) indicated a partial contribution of the ^2S_O conformation to the conformational equilibrium in the I_r residue. Unlike this, the H5−H2 cross-peak was not observed in the I_{nr} residue, which is in agreement with the presence of the unique $^1C_4$ form. Quantitative analysis of time-averaged NOEs obtained using the full relaxation matrix confirmed that the $^1C_4$:^2S_O ratio is approximately 80:20 (Table 2b). The computed glycosidic torsion angles for the structure that satisfied the experimental data are listed in Table 3.

Conformational Analysis of TETRA Bound to FGF2. Both the upfield and downfield shifts as well as the line width

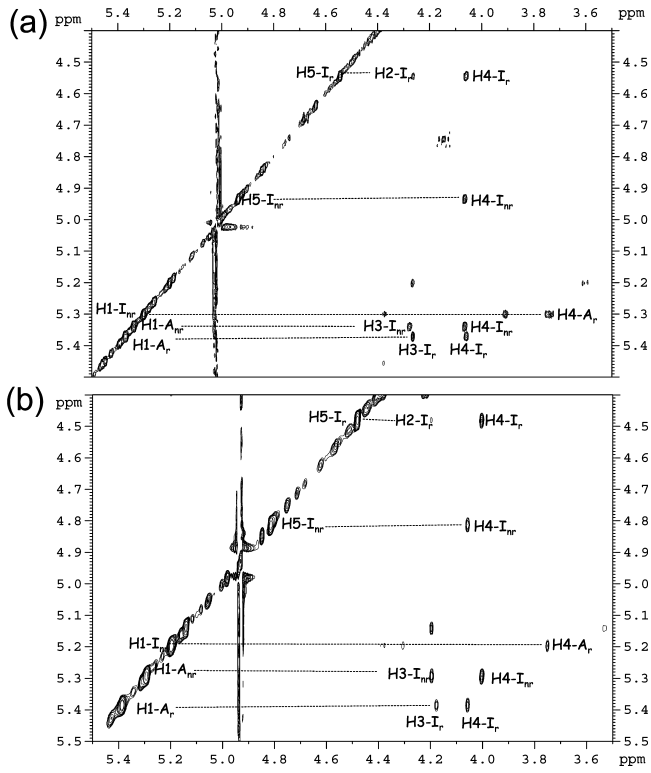

FIGURE 3: Partial NOE and tr-NOE spectra (750 MHz, 9 °C, mixing time of 300 ms) of TETRA in the free state (a) and bound to FGF2 (b). Dipolar correlations analyzed by CORCEMA are denoted with dashed lines.

increase of the proton resonances of the bound tetrasaccharide compared to its free state (Figure 2) indicated intermolecular interactions with FGF2. The evidence of these interactions was also supported by the changes in NOE magnitudes induced by FGF2 (Table 2a). Because of the large line widths, $^3J_{HH}$ coupling constants could not be determined from the ^{1}H NMR spectrum of the bound tetrasaccharide. The conformation of the tetrasaccharide in the bound state was resolved by quantitative analysis of tr-NOESY spectra, recorded at three different mixing times (100, 200, and 300 ms) (Figure 3b and Table 2a). Using the CORCEMA program to interpret the magnitudes of tr-NOEs and stochastic dynamics simulations (see Experimental Procedures), different models of the tetrasaccharide FGF2 complex were obtained. Furthermore, three different pyranose ring conformations (^2S_O, $^1C_4$, and $^4C_1$) of the I_r residue in the tetrasaccharide were considered in simulations to take into account all possible forms of the reducing end IdoA residue in the tetrasaccharide (Table 2b).

The agreement between the theoretical NOEs and the experimental tr-NOEs (Table 2) was evaluated by calculating *R* factors (see Experimental Procedures). Calculated tr-NOEs for protons cross-relaxing within the GlcN residues (e.g., $A1_{nr}$-$A2_{nr}$ and $A1_r$-$A2_r$) agreed well with experimental data in all three models. Similarly, most of the inter-residue NOEs for $A1_{nr}$-$I3_{nr}$, $A1_{nr}$-$I4_{nr}$, and $I1_{nr}$-$A4_r$ agreed (*R* factors ranging from 0.02 to 0.19), with the exception for $A1_{nr}$-$I3_{nr}$ NOEs of the model having I_r in the $^4C_1$ conformation ($R = 0.32$). The poor fitting of this last value might originate in the presence of more conformers with comparable energies due to the large low-energy plateau found in the potential energy map. This seems typical for the A-I glycosidic linkage in compounds having the iduronic moiety in the $^4C_1$ conformation (*37*). In the other models (^2S_O and $^4C_1$), both $A1_r$-$I3_r$ and $A1_r$-$I4_r$ tr-NOEs are much weaker than the experimental data ($R = 0.37-0.58$). Moreover, for the IdoA intraresidue NOEs, both $I5_{nr}$-$I4_{nr}$ and $I5_r$-$I4_r$ NOEs have comparable magnitudes, whereas I5r-$I2_r$ and $I5_{nr}$-$I2_{nr}$ NOEs are very small. Consequently, comparison between experimental and theoretical I5-I2 NOE magnitudes gives rise to *R* factors that are much higher than those calculated for other correlations.

The tetrasaccharide−FGF2 model in which I_{nr} and I_r were in the $^1C_4$ conformation best agreed with the experimental data. This model showed satisfactory agreement for the inter-residue tr-NOEs in the reducing end part of the tetrasaccharide (e.g., $A1_r$-$I3_r$ and $A1_r$ -$I4_r$; $R = 0.08$). Further, among the I5-I2 *R* factors, the theoretical NOEs of models having I_r in the $^1C_4$ chair conformation best fit with the experimental data. It is also important to note that the I5-I2 NOE magnitudes are at the limit of the experimental sensitivity. Thus, their experimental values could be overestimated and therefore produce higher *R* factors due to relatively large experimental errors that are expected for NOEs at the level of 1%. The computed torsion angles at the glycosidic linkages for the tetrasaccharide that was found as the best fit to the experimental data in the complex with FGF2 are listed in Table 3.

On the basis of earlier studies (*27*), which show that FGF2 binding induces a kink in the helical structure of the HSGAG oligosaccharide, local helical parameters (as described in ref *27*) were calculated for each disaccharide repeat unit (A_{nr}-I_{nr}, I_{nr}-A_r, and A_r-I_r) in the tetrasaccharides with I_r in the $^4C_1$, ^2S_O, or $^1C_4$ conformation. Given that the chain length is only a tetrasaccharide, it was challenging to quantify the formation of the kink as in the case of the FGF2−ΔHEXA cocrystal structure (*27*) (where the chain length is a hexasaccharide). However, there was a reduction in the axial distance per disaccharide observed for the A_{nr}-I_{nr}-A_r motif. This suggests the potential for this motif to form the kink in a larger oligosaccharide that is bound to FGF2. Furthermore, the modeled FGF2 tetrasaccharide complex where both I_{nr} and I_r are in the $^1C_4$ conformation showed the most optimal contacts in comparison with structures with other conformations of I_r such as $^4C_1$ and ^2S_O. The contacts were quantified by measuring the difference in the solvent accessible surface area [calculated using the Solvation module of InsightII (Accelrys, San Diego, CA)] of TETRA (with I_r in different ring conformations) in the free state and FGF2-bound state. The losses of solvent accessible surface area of 316.8, 249, and 169.25 Å^2 for the FGF2-bound TETRA where I_r is in $^1C_4$, ^2S_O, and $^4C_1$ conformations, respectively, showed that the $^1C_4$ conformation of I_r provides the most optimal contact with FGF2.

Comparison of the Modeled TETRA−FGF2 Complex with the Hexasaccharide−FGF2 Cocrystal Structure. The cocrystal structure of FGF2 with a 6-O-sulfated hexasaccharide ΔHEXA (*29*) comprises the internal tetrasaccharide motif, -$A_{NS,6S}$-I_{2S}-$A_{NS,6S}$-I_{2S}-, which is the 6-O-sulfated form of the tetrasaccharide TETRA used in this study (Figure 1). Superimposition of FGF2 in our modeled solution structure with that in the cocrystal structure provided insights into differences in HSGAG conformation and in the interactions of a 6-O-sulfated and nonsulfated HSGAG oligosaccharide with FGF2 (Figure 4).

Table 2: Selected Experimental NOE and tr-NOE Values of TETRA in Its Free State and Bound to FGF2 (9 °C, 750 MHz) (a), Selected Time-Averaged Theoretical NOE Values Based on Two Conformers of Free TETRA Differing in I_r Conformation (80:20 $^1C_4$:^2S_O ratio) (b), and Selected Theoretical NOE Values, Interproton Distances (r) and R Factors, Based on Three Molecular Models of the TETRA−FGF2 Complex Differing in I_r Conformation (c)[a]

(a)	free state		bound state		
proton pair	300 ms	150 ms	300 ms	200 ms	100 ms
$A1_{nr}$ $A2_{nr}$	5.9	3.4	12.0	8.2	3.5
$I3_{nr}$	4.9	2.2	10.6	6.8	3.3
$I4_{nr}$	6.1	2.8	15.1	9.8	4.8
$I5_{nr}$ $I4_{nr}$	6.2	3.1	13.1	9.2	4.9
$I2_{nr}$	0	0	2.8	1.4	0
$I1_{nr}$ $A4_r$	6.1	3.0	16.0	10.1	4.6
$A1_r$ $A2_r$	6.1	3.0	12.5	8.5	4.4
$I3_r$	4.0	1.8	10.5	6.5	3.1
$I4_r$	4.4	2.4	14.6	9.7	4.8
$I5_r$ $I4_r$	4.0	2.3	10.5	6.8	3.2
$I2_r$	1.7	1.0	3.5	2.1	0

(b)	free state	
proton pair	300 ms	150 ms
$A1_{nr}$ $A2_{nr}$	5.8	2.8
$I3_{nr}$	4.1	2.0
$I4_{nr}$	6.1	3.0
$I5_{nr}$ $I4_{nr}$	4.7	2.4
$I2_{nr}$	0	0
$I1_{nr}$ $A4_r$	5.5	2.7
$A1_r$ $A2_r$	4.5	2.2
$I3_r$	4.1	2.0
$I4_r$	4.2	2.1
$I5_r$ $I4_r$	5.1	2.6
$I2_r$	1.8	1.1

(c)	I_r, $^1C_4$ conformation					I_r, ^2S_O conformation					I_r, $^4C_1$ conformation				
proton pair	300 ms	200 ms	100 ms	r (Å)	R	300 ms	200 ms	100 ms	r (Å)	R	300 ms	200 ms	100 ms	r (Å)	R
$A1_{nr}$ $A2_{nr}$	12.5	8.2	4.1	2.41	**0.04**	10.6	7.1	3.6	2.46	**0.12**	10.8	8.3	3.8	2.41	**0.09**
$I3_{nr}$	10.8	7.0	3.4	2.47	**0.02**	9.4	6.3	3.2	2.49	**0.11**	7.2	4.8	2.4	2.69	**0.32**
$I4_{nr}$	14.0	9.3	4.7	2.34	**0.07**	12.1	8.2	4.3	2.38	**0.19**	11.8	8.2	4.3	2.35	**0.21**
$I5_{nr}$ $I4_{nr}$	12.9	8.2	4.0	2.44	**0.05**	11.5	7.5	3.8	2.45	**0.14**	11.2	7.5	3.8	2.43	**0.15**
$I2_{nr}$	1.1	0.7	0.3	3.92	**0.60**[b]	0.9	0.6	0.3	3.94	**0.67**[b]	1.0	0.6	0.3	3.90	**0.65**[b]
$I1_{nr}$ $A4_r$	15.8	10.8	5.5	2.24	**0.03**	12.7	8.8	4.6	2.33	**0.19**	13.7	9.6	5.1	2.26	**0.13**
$A1_r$ $A2_r$	12.5	8.3	4.1	2.38	**0.01**	11.3	0.5	3.7	2.48	**0.10**	12.1	8.2	4.1	2.41	**0.03**
$I3_r$	11.3	7.3	3.6	2.49	**0.08**	6.5	4.3	2.1	2.95	**0.37**	4.7	3.1	1.5	3.52	**0.55**
$I4_r$	13.5	9.0	4.5	2.32	**0.08**	6.6	4.4	2.2	2.85	**0.55**	6.1	4.1	2.1	2.92	**0.58**
$I5_r$ $I4_r$	12.7	8.2	4.0	2.43	**0.21**	12.4	8.4	4.4	2.34	**0.20**	11.2	7.4	3.7	2.46	**0.07**
$I2_r$	1.2	0.7	0.3	3.87	**0.67**[b]	11.9	7.9	4.0	2.26	**2.46**[b]	1.3	0.8	0.3	4.24	**0.63**[b]

[a] Poor fitting is outlined. [b] R factor calculated using two mixing times (300 and 200 ms).

Table 3: φ and ψ Dihedral Angles in Tetrasaccharide TETRA in the Free State (with I_r in both $^1C_4$ and ^2S_O forms) and in the Complex with FGF2[a]

	ΔU_{2S}-A (φ, ψ) (deg)	A_{nr}-I_{nr} (φ, ψ) (deg)	I_{nr}-A_r (φ, ψ) (deg)	A_r-I_r (φ, ψ) (deg)	I_r-$A_{NS,6S}$red (φ, ψ) (deg)
TETRA free, I_r $^1C_4$		−39, −21	37, 19	−42, −25	
TETRA free, I_r ^2S_O		−37, −23	18, 27	−57, −38	
TETRA−FGF2 (I_r $^1C_4$)		−37, −22	33, 18	−38, −22	
ΔHEXA	55, 9	−28, −5	55, 21	−39, −38	45, 24

[a] Dihedral angles in the cocrystal hexasaccharide ΔHEXA structure (*29*) are shown in the last row for comparison.

Comparison of the φ and ψ torsion angles in TETRA with those in ΔHEXA indicates that there are some differences in overall conformations between these two carbohydrates in their complex with protein (Table 3). The key difference between the NMR solution structure of TETRA and the cocrystal structure of ΔHEXA is that both I_{nr} and I_r of the tetrasaccharide in solution adopt the $^1C_4$ chair conformation whereas the corresponding IdoA residues of the hexasaccharide in the cocrystal structure adopt the $^1C_4$ and ^2S_O conformations, respectively.

Intermolecular distances between the protein and ligand polar groups were used to distinguish the FGF2−HSGAG interactions between the solution structures and the cocrystal structure (Table 4). The NS group of A_{nr} and the 2S group of I_{nr} in the solution structure of the TETRA−FGF2 complex have similar interactions with FGF2 as observed in the cocrystal structure of ΔHEXA. The $^1C_4$ conformation of I_{nr} in the solution structure is consistent with its role as a part of the structural recognition motif, A_{nr}-I_{nr}-A_r, that constitutes the kink in longer oligosaccharides bound to FGF2. On the other hand, there are significant differences in the contacts between I_r in the $^1C_4$ conformation (as in the solution structure of TETRA) and the corresponding IdoA in the ^2S_O conformation in the cocrystal structure of ΔHEXA. As illustrated in Figure 4, whereas the carboxylate group of this latter residue lies significantly far from Lys26 in the ΔHEXA cocrystal structure, I_r of TETRA makes strong contacts with

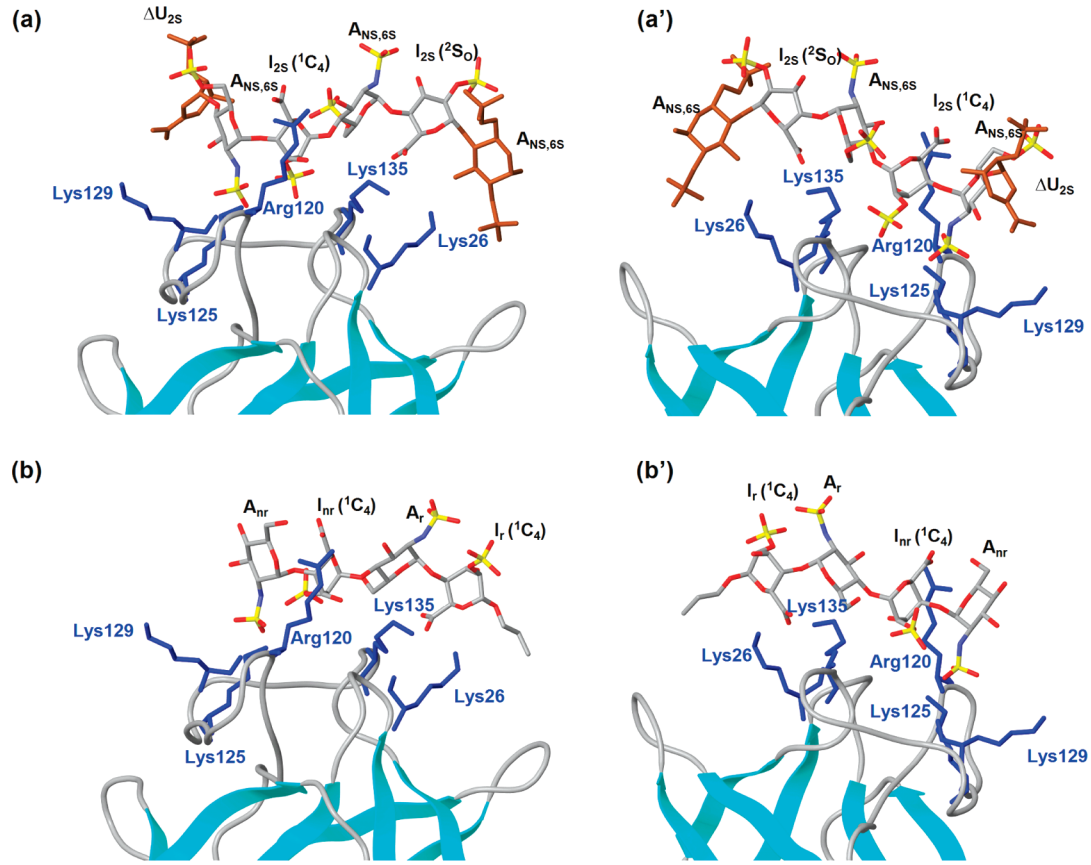

FIGURE 4: X-ray hexasaccharide ΔHEXA structure (a and a′) (*29*) and NMR tetrasaccharide TETRA (b and b′) structures in their complex with FGF2 viewed from opposite sides.

Table 4: Comparison between Polar Contacts Detected in the Hexasaccharide−FGF2 Cocrystal Structure and the Tetrasaccharide−FGF2 NMR Structure[a]

ligand polar group	FGF2 residue	FGF2 atom	ΔHEXA [distance (Å)]	TETRA [distance (Å)]
NS-A_{nr}	Arg120	NH	3.1	3.1
NS-A_{nr}	Lys125	Nζ	2.9	2.9
6COO-	Arg120	Nη1	3.1	3.2
2S-I_{nr}	Lys125	Nζ	3.0	3.3
2S-I_{nr}	Gln134	Nε2	3.4	4.7
2S-I_{nr}	Lys135	NH	3.1	4.4
2S-I_{nr}	Ala136	NH	3.0	5.3
O6-A_r	**Lys135**	**NH**	**5.7**	**4.8**
COO-I_r	Lys135	Nζ	3.3	4.4
COO-I_r	**Lys26**	**Nζ**	**4.4**	**2.8**
NS-$A_{NS,6Sred}$	Lys26	Nζ	3.6	
NS-$A_{NS,6Sred}$	Asn101	Nδ2	2.5	
3OH-$A_{NS,6Sred}$	Lys26	Nζ	2.8	

[a] Distances in bold were not listed in ref *29*.

such a lysine (Table 4). Further, the I_r residue is closer to the FGF2 binding pocket, and thus, its carboxylate group is positioned to make additional favorable contacts with the N and O atoms of the Gly133−Lys135 backbone. Thus, I_r in the $^1C_4$ conformation in the solution structure of TETRA is positioned to make more favorable contacts with FGF2 in comparison with the corresponding residue in the ^2S_O conformation in the cocrystal structure of ΔHEXA. Similarly, structural differences between the NMR structure of a synthetic hexasaccharide in the complex with FGF1 with respect to the corresponding crystal were found in a recent study (*19*).

DISCUSSION

The best-characterized examples of sequence−activity relationships in HSGAG−protein interactions are those of a specific pentasaccharide sequence (-$A_{NAc/NS,6S}$-G-$A_{NS,3S,6S}$-I_{2S}-$A_{NS,6S}$) within heparin which interacts with antithrombin (AT) and modulates heparin's anticoagulant activity, and the heparin and HS oligosaccharides that bind to FGF1 and FGF2 (*2, 46*). In the case of AT, the presence of a G residue in the $^4C_1$ conformation at the nonreducing end and the kink present in the -$A_{NS,3S,6S}$-I_{2S}-$A_{NS,6S}$- trisaccharide motif pattern (mainly associated with the axially oriented glycosidic bond of I_{2S} in the $^1C_4$ form) enhance the contacts of critical sulfate groups with the protein (*47, 27*). The NMR study also demonstrated that although the 2-sulfate group of the I_{2S} residue is not involved in the binding with AT, it is the driving force that influences the conformational equilibrium in the I_{2S} residue toward the skew form, increasing the structural specificity for protein binding (*47*).

The FGF−HSGAG interactions also require minimal chain lengths and sulfation patterns. Analysis of the FGF1−HSGAG (*28*) and FGF2−ΔHEXA (*29*) X-ray cocrystal structures points to important similarities and differences in the interactions of these FGFs with the HSGAGs. The N and 2-O sulfate groups in the HSGAGs are important for interactions with both FGF1 and FGF2, consistent with other studies (*16, 48, 49*). Furthermore, these sulfate groups are a part of the trisaccharide kink motif $A_{NS,6X}$-I_{2S}-$A_{NS,6X}$ that provides maximum contact with the HSGAG binding site on the FGFs (*27*). There are significant differences between the contacts of the 6-O-sulfate group of the HSGAG with FGF1 and FGF2. In the complex with FGF1, the $A_{NS,6S}$

residue following I_{2S} in the kink motif interacts with the protein also through its 6S group (*27, 53*). On the other hand, in the complex with FGF2 (*29, 53*) the 6S group of the analogous $A_{NS,6S}$ residue is not involved in the contacts with FGF2 (Figure 4). In fact, differences in the orientation of this 6S group in the FGF1− and FGF2−HSGAG cocrystal structures can be observed. In the FGF1−HSGAG cocrystal structure (*28*), the dihedral angle ω (O5−C5−O6−C6), describing the orientation of this 6S group, is around −60°, indicating a "gauche-gauche" conformation. On the other hand, in the ΔHEXA−/FGF2 crystal structure (*29*) the dihedral angle ω (O5−C5−O6−C6) has a value of ∼0°. In this orientation, the 6-O-sulfate group faces away from the HSGAG binding site on FGF2, thereby preventing its direct contribution to the interaction.

In this study, we demonstrated by high-resolution NMR and molecular modeling that a non-6-O-sulfated tetrasaccharide (TETRA) constitutes the shortest non-6-O-sulfate oligosaccharide interacting with the heparin and heparan sulfate binding region of FGF2. While such an assumption will be validated by ongoing studies, these results further confirm differences in the role of 6-O-sulfate groups in the interaction with FGF1 and FGF2. Comparison of the solution structure of the FGF2−TETRA complex and the cocrystal structure of the FGF2−ΔHEXA complex permitted us to point out that the conformational flexibility of IdoA residues provides the necessary specificity of FGF binding in the presence or absence of 6S groups. The structural differences between TETRA and ΔHEXA, involving both the chain length and sulfation pattern, affect the conformation of their iduronate moieties both in the free state solution and in FGF2-bound state. The relative $^1C_4$:^2S_O population of both I_{2S} residues (analogous to I_{nr} and I_r in the TETRA) of free ΔHEXA was calculated to be ∼70:30 (*31*). On the other hand, the I_{nr} in free TETRA is present almost exclusively in the $^1C_4$ conformation and the ^2S_O form contributes to the conformational equilibrium of the reducing end IdoA (I_r) by ∼20% (*26, 44*). These observations indicate that the absence of the 6-O-sulfate group in TETRA drives the IdoA conformation to $^1C_4$ in the free state, and this conformation is able to contribute to the optimal molecular fit between TETRA and FGF2.

Although the 6-O-sulfate group is not directly involved in binding to FGF2, this group has been demonstrated to play a critical role in bridging the FGF2−FGF receptor complexes and thus is essential for FGF2-mediated signaling (*51, 52*). The position of the minimal binding site (in the presence or absence of 6S along an oligosaccharide chain) could therefore dictate the formation of an active or inactive signaling complex, thereby explaining both activating and inhibitory roles of HSGAGs in FGF signaling. In other words, the presence of an additional 6S group in the context of the minimal binding requirements could play a key role in distinguishing FGF2 binding and assembling FGF2−FGFR complexes on the cell surface for active signaling. Recent studies support the functional importance of the 6S group in FGF2 in tumor growth. These studies have shown that *Hsulf-1* and *Hsulf-2* (endo 6S desulfatase) are downregulated in tumor cells and that the expression of these enzymes in tumor cells significantly inhibits tumor growth and progression potentially by interfering with FGF signaling (*54*).

ACKNOWLEDGMENT

The 750 MHz spectra were recorded at the SON NMR Large Scale Facility in Utrecht, which is funded by the 'Access to Research Infrastructures' program of the European Union (HPRI-CT-1999-00005 and HPRI-CT-2001-00172). We thank Dr. Edwin A. Yates for useful discussions.

REFERENCES

1. Conrad, H. E. (1998) *Heparin-Binding Proteins*, Academic Press, San Diego.
2. Casu, B., and Lindahl, U. (2001) Structure and biological interactions of heparin and heparan sulfate. *Adv. Carbohydr. Chem. Biochem. 57*, 159–206.
3. Esko, J. D., and Selleck, S. B. (2002) Order out of chaos: Assembly of ligand binding sites in heparan sulfate. *Annu. Rev. Biochem. 71*, 435–471.
4. Lindahl, U., Kusche-Gullberg, M., and Kjellén, L. (1998) Regulated diversity of heparan sulfate. *J. Biol. Chem. 273*, 24979–24982.
5. Tumova, S., Woods, A., and Couchman, J. R. (2000) Heparan sulfate proteoglycans on the cell surface: Versatile coordinators of cellular functions. *Int. J. Biochem. Cell Biol. 32*, 269–288.
6. Capila, I., and Linhardt, R. J. (2002) Heparin-protein interactions. *Angew. Chem., Int. Ed. 41*, 391–412.
7. Sasisekharan, R., Raman, R., and Prabhakar, V. (2006) Glycomics approach to structure-function relationships of glycosaminoglycans. *Annu. Rev. Biomed. Eng. 8*, 181–231.
8. Lin, X. (2004) Functions of heparan sulfate proteoglycans in cell signaling during development. *Development 131*, 6009–6021.
9. Perrimon, N., and Bernfield, M. (2000) Specificities of heparan sulphate proteoglycans in developmental processes. *Nature 404*, 725–728.
10. Yayon, A., Klagsbrun, M., Esko, J. D., Leder, P., and Ornitz, D. M. (1991) Cell surface, heparin-like molecules are required for binding basic fibroblast growth factor to its high affinity receptor. *Cell 64*, 841–848.
11. Venkataraman, G., Raman, R., Sasisekharan, V., and Sasisekharan, R. (1999) Molecular characteristics of fibroblast growth factor−fibroblast growth factor receptor-heparin-like glycosaminoglycan complex. *Proc. Natl. Acad. Sci. U.S.A. 96*, 3658–3663.
12. Sasisekharan, R., Shriver, Z., Venkataraman, G., and Narayanasami, U. (2002) Roles of heparan sulfate glycosaminoglycans in cancer. *Nat. Rev. Cancer 2*, 521–528.
13. Humphries, D. E., Wong, G. W., Friend, D. S., Gurish, M. F., Qiu, W. T., Huang, C., Sharpe, A. H., and Stevens, R. L. (1999) Heparin is essential for the storage of specific granule proteases in mast cells. *Nature 400*, 769–772.
14. Iozzo, R. V., and San Antonio, J. D. (2001) Heparan sulfate proteoglycans: Heavy hitters in the angiogenesis arena. *J. Clin. Invest. 108*, 349–355.
15. Delehedde, M., Lyon, M., Gallagher, J. T., Rudland, P. S., and Fernig, D. G. (2002) Fibroblast growth factor-2 binds to small heparin-derived oligosaccharides and stimulates a sustained phosphorylation of p42/44 mitogen-activated protein kinase and proliferation of rat mammary fibroblasts. *Biochem. J. 366*, 235–244.
16. Mohammadi, M., Olsen, S. K., and Ibrahimi, O. A. (2005) Structural basis for fibroblast growth factor receptor activation. *Cytokine Growth Factor Rev. 16*, 107–137.
17. Pellegrini, L. (2001) Role of heparan sulfate in fibroblast growth factor signaling: A structural view. *Curr. Opin. Struct. Biol. 11*, 629–634.
18. Canales, A., Angulo, J., Ojeda, R., Bruix, M., Fayos, R., Lozano, R., Gimenez-Gallego, G., Martin-Lomas, M., Nieto, P. M., and Jimenez-Barbero, J. (2005) Conformational flexibility of a synthetic glycosylaminoglycan bound to a fibroblast growth factor. FGF-1 recognizes both the C-1 (4) and S-2 (0) conformations of a bioactive heparin-like hexasaccharide. *J. Am. Chem. Soc. 127*, 5778–5779.
19. Canales, A., Lozano, R., Lopez-Mendez, B., Angulo, J., Ojeda, R., Nieto, P. M., Martin-Lomas, M., Gimenez-Gallego, G., and Jimenez-Barbero, J. (2006) Solution NMR structure of a human FGF-1 monomer, activated by a hexasaccharide heparin-analogue. *FEBS J. 20*, 4716–4721.
20. Coltrini, D., Rusnati, M., Zoppetti, G., Oreste, P., Isacchi, A., Caccia, P., Bergonzoni, L., and Presta, M. (1993) Biochemical bases of the interaction of human fibroblast growth factor with glycosaminoglycans. *Eur. J. Biochem. 214*, 51–58.

21. Venkataraman, G., Shriver, Z., Davis, J. C., and Sasisekharan, R. (1999) Fibroblast growth factors 1 and 2 are distinct in oligomerization in the presence of heparin-like glycosaminoglycans. *Proc. Natl. Acad. Sci. U.S.A. 96*, 1892–1897.
22. Coltrini, D., Rusnati, M., Zoppetti, G., Oreste, P., Grazioli, G., Naggi, A., and Presta, M. (1994) Different effects of mucosal, bovine lung and chemically modified heparin on selected biological properties of basic fibroblast growth factor. *Biochem. J. 303*, 583–590.
23. Mulloy, B., and Forster, M. J. (2000) Conformation and dynamics of heparin and heparan sulfate. *Glycobiology 10*, 1147–1156.
24. Nieduszynski, I. A. (1985) Connective tissue polysaccharides. In *Polysaccharides: Topics in structure and morphology* (Atkins, E. D. T., Ed.) pp 107−139, McMillian, London.
25. Casu, B., Choay, J., Ferro, D. R., Gatti, G., Jacquinet, J. C., Petitou, M., Provasoli, A., Ragazzi, M., Sinay, P., and Torri, G. (1986) Controversial glycosaminoglycan conformations. *Nature 322*, 215–216.
26. Ferro, D. R., Provasoli, A., Ragazzi, M., Casu, B., Torri, G., Bossennec, V., Perly, B., Sinay, P., Petitou, M., and Choay, J. (1990) Conformer populations of L-iduronic acid residues in glycosaminoglycan sequences. *Carbohydr. Res. 195*, 157–167.
27. Raman, R., Venkataraman, G., Ernst, S., Sasisekharan, V., and Sasisekharan, R. (2003) Structural specificity of heparin binding in the fibroblast growth factor family of proteins. *Proc. Natl. Acad. Sci. U.S.A. 100*, 2357–2362.
28. DiGabriele, A. D., Lax, I., Chen, D. I., Svahn, C. M., Jaye, M., Schlessinger, J., and Hendrickson, W. A. (1998) Structure of a heparin-linked biologically active dimer of fibroblast growth factor. *Nature 393*, 812–817.
29. Faham, S., Hileman, R. E., Fromm, J. R., Linhardt, R. J., and Rees, D. C. (1996) Heparin structure and interactions with basic fibroblast growth factor. *Science 271*, 1116–1120.
30. Kreuger, J., Salmivirta, M., Sturiale, L., Gimenez-Gallego, G., and Lindahl, U. (2001) Sequence analysis of heparan sulfate epitopes with graded affinities for fibroblast growth factors 1 and 2. *J. Biol. Chem. 276*, 30744–30752.
31. Mikhailov, D., Linhardt, R. J., and Mayo, K. H. (1997) NMR solution conformation of heparin-derived hexasaccharide. *Biochem. J. 328*, 51–61.
32. Poletti, L., Lay, L., Fleischer, M., Vogel, C., Guerrini, M., Torri, G., and Russo, G. A. (2001) Rational approach to heparin-related fragments. Synthesis of differently sulfated tetrasaccharides as potential ligands toward fibroblast growth factors. *Eur. J. Org. Chem. 14*, 2727–2734.
33. Guerrini, M., Agulles, T., Bisio, A., Hricovini, M., Lay, L., Naggi, A., Poletti, L., Sturiale, L., Torri, G., and Casu, B. (2002) Minimal heparin/heparan sulfate sequences for binding fibroblast growth factor 1. *Biochem. Biophys. Res. Commun. 292*, 222–230.
34. Homans, S. W. (1990) A molecular mechanical force field for the conformational analysis of oligosaccharides: Comparison of theoretical and crystal structures of Man-α1,3-Man-β1,4-GlcNAc. *Biochemistry 29*, 9110–9118.
35. Still, W. C., Tempczyk, A., Hawley, R. C., and Hendrickson, T. (1990) A general treatment of solvation for molecular mechanics. *J. Am. Chem. Soc. 112*, 6127–6129.
36. Mulloy, B., Forster, M. J., Jones, C., and Davies, D. B. (1993) N.M.R. and molecular-modelling studies of the solution conformation of heparin. *Biochem. J. 293*, 849–858.
37. Chang, G., Guida, W. C., and Still, W. C. (1989) An internal-coordinate Monte Carlo method for searching conformational space. *J. Am. Chem. Soc. 111*, 4379–4386.
38. Goodman, J. M., and Still, W. C. (1991) An unbounded systematic search of conformational space. *J. Comput. Chem. 12*, 1110–1117.
39. Cros, S., Petitou, M., Sizun, P., Perez, S., and Imberty, A. (1997) Combined NMR and molecular modeling study of an iduronic acid-containing trisaccharide related to antithrombotic heparin fragments. *Bioorg. Med. Chem. 5*, 1301–1309.
40. Ragazzi, M., Ferro, D. R., Perly, B., Sinay, P., Petitou, M., and Choay, J. (1990) Conformation of the pentasaccharide corresponding to the binding site of heparin for antithrombin III. *Carbohydr. Res. 195*, 169–185.
41. Moseley, H. N., Curto, E. V., and Krishna, N. R. (1995) Complete relaxation and conformational exchange matrix (CORCEMA) analysis of NOESY spectra of interacting systems; two-dimensional transferred NOESY. *J. Magn. Reson., Ser. B 108*, 243–261.
42. Moy, F. J., Safran, M., Seddon, A. P., Kitchen, D., Bohlen, P., Aviezer, D., Yayon, A., and Powers, R. (1997) Properly oriented heparin-decasaccharide-induced dimers are the biologically active form of basic fibroblast growth factor. *Biochemistry 36*, 4782–4791.
43. Ferro, D. R., Provasoli, A., Ragazzi, M., Torri, G., Casu, B., Gatti, G., Jacquinet, J. C., Sinay, P., Petitou, M., and Choay, J. (1986) Evidence for conformational equilibrium of the sulfated L-iduronate residue in heparin and in synthetic mono- and oligosaccharides. *J. Am. Chem. Soc. 108*, 6773–6778.
44. Hricovíni, M., and Bízik, F. (2007) Relationship between structure and three-bond proton−proton coupling constants in glycosaminoglycans. *Carbohydr. Res. 342*, 779–783.
45. Hricovíni, M. (2006) B3LYP/6-311++G** study of structure and spin-spin coupling constant in methyl 2-*O*-sulfo-α-L-iduronate. *Carbohydr. Res. 341*, 2575–2580.
46. Guerrini, M., Hricovíni, M., and Torri, G. (2007) Interaction of heparins with fibroblast growth factors: Conformational aspects. *Curr. Pharm. Des. 13*, 2045–2056.
47. Hricovíni, M., Guerrini, M., Bisio, A., Torri, G., Petitou, M., and Casu, B. (2001) Conformation of heparin pentasaccharide bound to antithrombin III. *Biochem. J. 359*, 265–272.
48. Turnbull, J. E., Fernig, D. G., Ke, Y., Wilkinson, M. C., and Gallagher, J. T. (1992) Identification of the basic fibroblast growth factor binding sequence in fibroblast heparan sulfate. *J. Biol. Chem. 267*, 10337–10341.
49. Wang, F., Kan, M., McKeehan, K., Jang, J. H., Feng, S., and McKeehan, W. L. (1997) A homeo-interaction sequence in the ectodomain of the fibroblast growth factor receptor. *J. Biol. Chem. 272* (38), 23887–23895.
50. Maccarana, M., Casu, B., and Lindahl, U. (1993) Minimal sequence in heparin-heparan sulfate required for binding of basic fibroblast growth factor. *J. Biol. Chem. 268*, 23898–23905.
51. Pye, D. A., Vives, R. R., Hyde, P., and Gallagher, J. T. (2000) Regulation of FGF-1 mitogenic activity by heparan sulfate oligosaccharides is dependent on specific structural features: Differential requirements for the modulation of FGF-1 and FGF-2. *Glycobiology 10*, 1183–1192.
52. Guimond, S., Maccarana, M., Olvin, B. B., Lindahl, U., and Rapraeger, A. C. (1993) Activating and inhibitory heparin sequences for FGF-2 (basic FGF). *J. Biol. Chem. 268*, 23906–23914.
53. Faham, S., Linhardt, R. J., and Rees, D. C. (1998) Diversity does make a difference: Fibroblast growth factor-heparin interactions. *Curr. Opin. Struct. Biol. 8*, 578–586.
54. Dai, Y., Yang, Y., MacLeod, V., Yue, X., Rapraeger, A. C., Shriver, Z., Venkataraman, G., Sasisekharan, R., and Sanderson, R. D. (2005) Hsulf-1 and Hsulf-2 are potent inhibitors of myeloma tumor growth in vivo. *J. Biol. Chem. 280*, 40066–40073.

BI801007P